Sensors and Materials, Vol. 33, No. 6 (2021) 2209–2214
MYU Tokyo

S & M 2609

Photo- and Radioluminescence Properties of Ce^{3+}-doped $Lu_3Al_5O_{12}$ Thick Film Grown by Chemical Vapor Deposition

Shogen Matsumoto,[1] Akihiro Minamino,[2] and Akihiko Ito[1*]

[1]Graduate School of Environment and Information Sciences, Yokohama National University,
79-7, Tokiwadai, Hodogaya-ku, Yokohama, Kanagawa 240-8501, Japan
[2]Graduate School of Engineering Science, Yokohama National University,
79-5 Tokiwadai, Hodogaya-ku, Yokohama, Kanagawa 240-8501, Japan

(Received January 31, 2021; accepted April 28, 2021)

Keywords: $Lu_3Al_5O_{12}$, chemical vapor deposition, thick film phosphor, scintillator, luminescence

We demonstrate the rapid synthesis of Ce^{3+}-doped $Lu_3Al_5O_{12}$ (Ce^{3+}:LuAG) thick film phosphor grown by laser-assisted chemical vapor deposition. The radioluminescence properties of the film are compared with those of Ce^{3+}:LuAG single crystals. The (100) Ce^{3+}-LuAG thick film was epitaxially grown on a (100) $Y_3Al_5O_{12}$ substrate at a deposition rate of 16 nm s^{-1}. Under UV and X-ray irradiation, the film emitted a yellow-green light originating from 5d–4f transitions of Ce^{3+} ions. Under α-ray excitation from an ^{241}Am source, the scintillation decay curve of the Ce^{3+}:LuAG thick film was fitted to two time constants, 32 and 666 ns, associated with the Ce^{3+} centers and antisite defects in garnet structures, respectively.

1. Introduction

Radiation imaging systems are employed in medical radiography, security checks, environmental measurements, and high-energy physics.[1–5] In these imaging techniques, high-energy radiation is detected by photodiodes or charge-coupled detectors with Tl^+-doped CsI film or Tb^{3+}-doped Gd_2O_2S powder phosphors.[6,7] However, the performance of current film phosphors is degraded by hygroscopicity and low spatial resolution. An alternative candidate material is $Lu_3Al_5O_{12}$ (LuAG), a novel scintillation material with a high relative density (6.73 Mg m^{-3}) and large effective atomic number (Z_{eff} = 61.7). By virtue of these properties, LuAG effectively blocks high-energy radiation.[8]

Ce^{3+}-doped LuAG generates a high light yield (25000 Ph MeV^{-1}) with a fast decay time (50–70 ns) owing to the allowed 5d–4f transitions of Ce^{3+} ions.[8,9] Ce^{3+}:LuAG films formed by pulsed laser deposition (PLD) are only 140 nm thick,[10] insufficient for blocking radiation. According to the Bragg–Kleeman law,[11,12] protective LuAG films against 4–8 MeV α radiation must be 3–13 μm thick. Fabricating such thick film phosphors by PLD is prohibitively time-consuming.

*Corresponding author: e-mail: ito-akihiko-xr@ynu.ac.jp
https://doi.org/10.18494/SAM.2021.3325

ISSN 0914-4935

Metal–organic chemical vapor deposition (MOCVD) is a promising process for growing thick films because it can synthesize functional ceramics at a high deposition rate (10–300 μm h^{-1}).[13,14] We have prepared transparent thick films of HfO_2 and Lu_2O_3 phosphors and $Y_3Fe_5O_{12}$ and $SrFe_{12}O_{19}$ magneto-optic crystals by the MOCVD technique.[15–18] In addition, the high dopant concentration with low segregation during vapor deposition will generate sufficient light intensity.

The present study demonstrates the high-speed epitaxial growth of Ce^{3+}:LuAG thick film phosphor. The growth mode, microstructure, and photo- and radioluminescence properties of the film are examined, and the scintillation properties of the obtained thick film phosphor are compared with those of Ce^{3+}:LuAG single crystals.

2. Materials and Methods

The laser-assisted CVD apparatus has been described elsewhere.[19] Metal–organic compounds of lutetium tris(dipivaloylmethanate) (Strem Chemicals, Inc., USA), aluminum tris(acetylacetonate) (Sigma-Aldrich Co. LLC, USA), and cerium tetrakis(dipivaloylmethanate) (Toshima Manufacturing Co., Ltd., Japan) were maintained at temperatures of 453, 453, and 493 K, respectively, in the precursor furnaces. The resultant vapor was transferred to the CVD chamber using Ar (purity: 99.9999%) as the carrier gas, and O_2 gas (99.5%) was separately introduced to the chamber through a double-tubed nozzle. The molar ratio in the precursor vapor was estimated from the mass change in each precursor before and after deposition, and it was calculated to be Ce:Lu:Al = 3:33:64 (9 mol%Ce). The total chamber pressure was maintained at 0.2 kPa.

The substrate was (100) $Y_3Al_5O_{12}$ (YAG; 5 × 5 × 0.5 mm^3) polished on both sides. The substrate was preheated to 1000 K on a heating stage, then irradiated with a CO_2 laser (wavelength: 10.6 μm; maximum laser output: 60 W; SPT Laser Technology Co., Ltd., China) through a ZnSe window. The laser irradiation heated the substrate to 1193 K. The deposition time was 0.3 ks.

The phase composition of the resultant film was determined by X-ray diffraction (XRD; Bruker D2 Phaser, USA), and the in-plane orientation was studied by X-ray pole figure measurements (Rigaku Ultima IV, Japan). The microstructure was observed using a scanning electron microscope (SEM; JEOL JCM-6000, Japan). An energy dispersive X-ray spectrometer attached with a SEM (SEM-EDX; JEOL JSM-6510LA) was used to determine the composition of the films. The in-line transmittance was measured using a UV–visible spectrophotometer (JASCO V-630, Japan) in the 190–1100 nm wavelength range. The photoluminescence (PL) and PL excitation (PLE) spectra were measured using fluorescence spectrophotometers (JASCO FP-8300 and FP-8500, Japan).

The X-ray-excited luminescence spectra were recorded using a spectrometer (Ocean Insights HR2000+, USA) under Cu Kα irradiation generated at 40 kV and 40 mA. Under α-ray excitation from a sealed source of ^{241}Am, the scintillation decay curves were measured in a photomultiplier tube (PMT; Hamamatsu Photonics R329-02, Japan) connected to an oscilloscope (Keysight DSOX3034T, USA). For this purpose, the specimens were mounted on the window of the PMT

with a thin layer of optical silicone grease (Adhesive Materials Group, V-788, USA). For comparison, a commercially available Ce^{3+}:LuAG single crystal (5 × 5 × 1 mm^3, Epic Crystal Co., Ltd., China) was evaluated in the same setup.

3. Results and Discussion

The out-of-plane XRD pattern of the resultant film was indexed to the LuAG structure (ICSD No. 182354; space group: $Ia\bar{3}d$ and a = 1.193 nm) with a (100) orientation [Fig. 1(a)]. X-ray pole figures of the LuAG {110} and YAG {110} planes presented fourfold patterns at the same azimuthal angle [Fig. 1(b)]. The in-plane orientation relationship was [001] Ce^{3+}:LuAG ‖ [001] YAG.

Figure 2 shows cross-sectional and surface SEM images of the Ce^{3+}:LuAG film grown on the YAG substrate. The cross section of the Ce^{3+}:LuAG film exhibited a dense structure with a smooth surface. The film was 4.8 μm thick, implying a deposition rate of 16 nm s^{-1}. The Ce molar content in the film was measured to be 5 mol%. The Ce^{3+}:LuAG film was transparent and

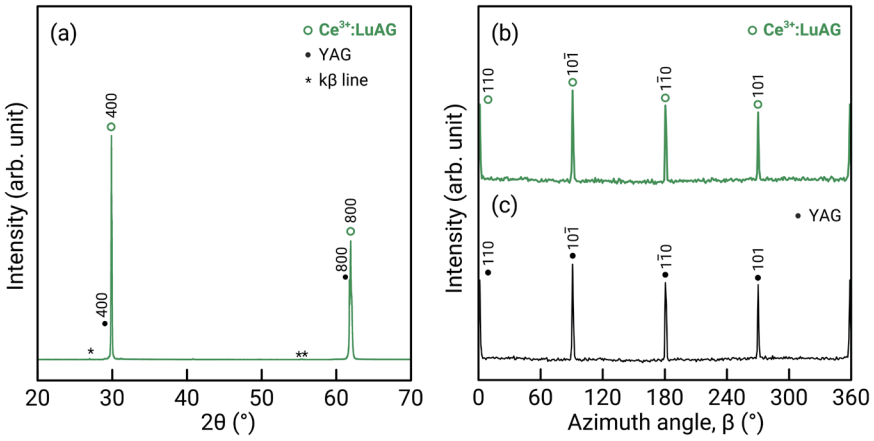

Fig. 1. (Color online) (a) Out-of-plane XRD pattern of Ce^{3+}:LuAG film prepared on (100) YAG substrate, and in-plane XRD patterns of (b) LuAG {110} plane and (c) YAG {110} plane.

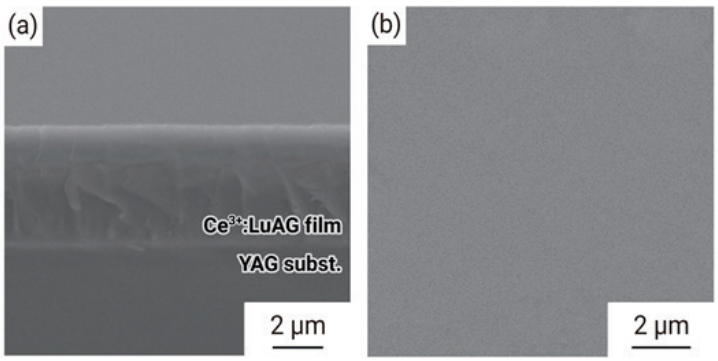

Fig. 2. (a) Cross-sectional and (b) surface SEM images of (100) Ce^{3+}:LuAG thick film epitaxially grown on YAG substrate.

yellowish-green (Fig. 3, inset). Its in-line transmittance was 63% that of the raw substrate, as depicted in Fig. 3.

Figure 4 shows the PL–PLE contour plots of the Ce^{3+}:LuAG film grown on the YAG substrate. The broad emission peak in the 500–600 nm range was attributed to $5d \rightarrow {}^2F_{5/2}$ and $5d \rightarrow {}^2F_{7/2}$ transitions of Ce^{3+} ions. The excitation bands around 250, 340, and 450 nm were contributed by energy transitions from the ground state (4f) to ${}^2T_{2g}$, ${}^2E_2$, and ${}^2E_1$, respectively. The Ce^{3+}:LuAG film grown on the YAG substrate emitted intense yellow-green emission under UV light irradiation from a low-pressure mercury-vapor lamp (Fig. 4, inset). The weak emission peak at 590 nm was attributed to ${}^5D_0 \rightarrow {}^7F_1$ transitions of Eu^{3+} ions, which were probably contaminants from the CVD chamber.

Figure 5 shows the scintillation spectra of the Ce^{3+}:LuAG film and a Ce^{3+}:LuAG single crystal under X-ray irradiation. Both samples produced a broad emission (at 470–650 nm) from 5d–4f transitions of Ce^{3+} ions. In the spectrum of the Ce^{3+}:LuAG film, the two broad peaks at 310 and 380 nm were associated with defect-related emission from LuAG and YAG hosts[20] and the sharp peaks around 590–620 nm were attributed to Eu^{3+} contamination.[21]

Figure 6 shows the scintillation decay curves under α-ray excitation of the Ce^{3+}:LuAG film and Ce^{3+}:LuAG single crystal. The decay curves of the Ce^{3+}:LuAG film and single crystal were both fitted to two decay time constants: 32 and 666 ns for the film and 55 and 768 ns for the crystal. The fast and slow decay time constants have been attributed to Ce^{3+} centers (50–70 ns) and Lu_{Al} antisite defects (600–1000 ns), respectively.[8] The fast decay constant of the grown film was lower than that in the single crystals (50–70 ns) and was comparable to that of the thin film (33 ns).[22] Because dopant elements can be more concentrated in films (10 mol%Ce in a previous study[22] and 5 mol%Ce in the present study) than in single crystals (0.03–0.12 mol%Ce),[23] the short lifetime of the Ce^{3+} centers in the film was attributed to Ce^{3+}-concentration quenching.[22]

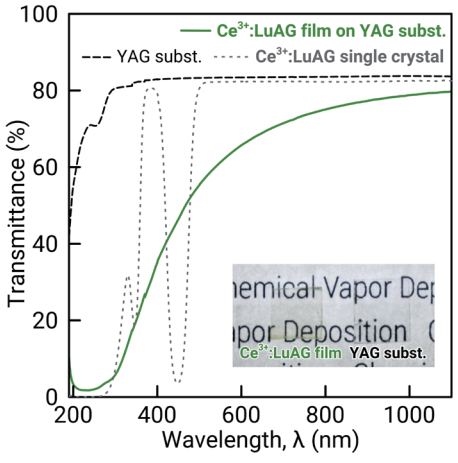

Fig. 3. (Color online) In-line transmittance spectra of Ce^{3+}:LuAG thick film epitaxially grown on YAG substrate (solid line), as-received YAG substrate (dashed line), and Ce^{3+}:LuAG single crystal (dotted line). The inset is a photograph of the film and its substrate.

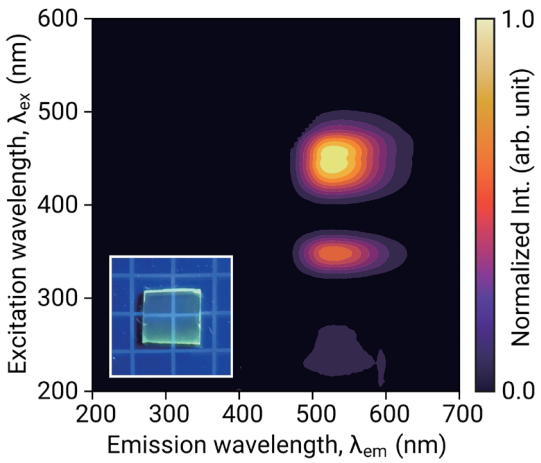

Fig. 4. (Color online) PL–PLE contour plots of Ce^{3+}- LuAG film epitaxially grown on YAG substrate. The inset is a photograph of the Ce^{3+}-doped LuAG thick film under UV irradiation (λ = 365 nm).

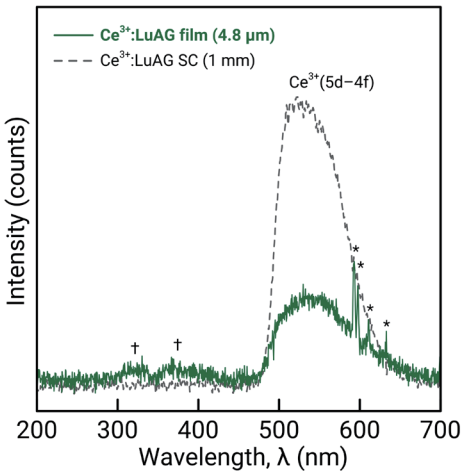

Fig. 5. (Color online) X-ray-induced scintillation spectra of Ce^{3+}:LuAG thick film and Ce^{3+}:LuAG single crystal. † and * indicate emissions from defects in LuAG and YAG hosts and Eu^{3+} contamination, respectively.

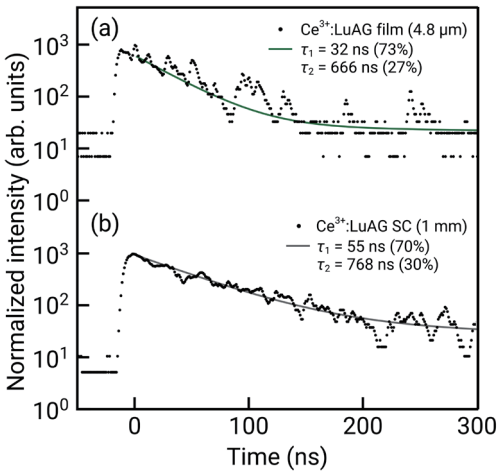

Fig. 6. Scintillation decay curves under α-ray irradiation from an ^{241}Am source: (a) Ce^{3+}:LuAG thick film epitaxially grown on YAG substrate and (b) Ce^{3+}:LuAG single crystal.

4. Conclusions

We synthesized Ce^{3+}:LuAG thick film phosphor on a (100) YAG substrate by laser-assisted CVD. The (100) Ce^{3+}:LuAG film was epitaxially grown on the (100) YAG substrate with an in-plane orientation relationship of [001] LuAG ‖ [001] YAG, and the deposition rate reached 16 nm s^{-1}. Under UV and X-ray irradiation, the Ce^{3+}:LuAG thick film emitted yellow-green light at 470–650 nm, originating from 5d–4f transitions of the Ce^{3+} centers. The scintillation decay curve of the Ce^{3+}:LuAG film was fitted to two time constants, 32 and 666 ns.

Acknowledgments

This study was supported in part by JSPS KAKENHI Grant Numbers JP17H03426, JP20H02477, and JP20H05186. This study was also supported by Yokohama Kogyokai, "Joint Research Project C" from the Graduate School of Environment and Information Sciences, Yokohama National University, and the Sasakawa Scientific Research Grant from The Japan Science Society. X-ray pole measurement (Ultima IV), energy dispersive X-ray spectrometer (JSM-6510LA), and fluorescence spectroscopy (FP-8500) were carried out at the Instrumental Analysis Center, Yokohama National University. S.M. would like to thank the Futaba Foundation for the financial assistance.

References

1 C. W. E. van Eijk: Phys. Med. Biol. **47** (2002) R85. https://doi.org/10.1088/0031-9155/47/8/201
2 D. R. Schaart, H. T. van Dam, S. Seifert, R. Vinke, P. Dendooven, H. Löhner, and F. J. Beekman: Phys. Med. Biol. **54** (2009) 3501. https://doi.org/10.1088/0031-9155/54/11/015

3 J. Glodo, Y. Wang, R. Shawgo, C. Brecher, R. H. Hawrami, J. Tower, and K. S. Shah: Phys. Procedia **90** (2017) 285. https://doi.org/10.1016/j.phpro.2017.09.012
4 S. Yamamoto and H. Tomita: Radiat. Meas. **115** (2018) 13. https://doi.org/10.1016/j.radmeas.2018.05.009
5 B. A. Shwartz: Engineering of Scintillation Materials and Radiation Technologies, Springer Proceedings in Physics (2016). https://doi.org/10.1007/978-3-319-68465-9_13
6 T. Martin and A. Koch: J. Synchrotron Radiat. **13** (2006) 180. https://doi.org/10.1107/S0909049506000550
7 B. K. Cha, J.-H. Shin, J. Y. Kim, H. Jeon, J. H. Bae, C.-H. Lee, S. Chang, H. Kim, B.-J. Kim, and G. Cho: 2008 IEEE Nuclear Science Symp. Conf. Record (2008). https://doi.org/10.1109/NSSMIC.2008.4774627
8 M. Nikl, A. Yoshikawa, K. Kamada, K. Nejezchleb, C. R. Stanek, J. A. Mares, and K. Blazek: Prog. Cryst. Growth Charact. Mater. **59** (2013) 47. https://doi.org/10.1016/j.pcrysgrow.2013.02.001
9 A. G. Petrosyan, K. L. Ovanesyan, R. V. Sargsyan, G. O. Shirinyan, D. Abler, E. Auffray, P. Lecoq, C. Dujardin, and C. Pedrini: J. Cryst. Growth **312** (2010) 3136. https://doi.org/10.1016/j.jcrysgro.2010.07.042
10 T. Zorenko, V. Gorbenko, T. Vozniak, S. Heinrich, G. Huber, and Yu. Zorenko: Opt. Mater. **105** (2020) 109751. https://doi.org/10.1016/j.optmat.2020.109751
11 W. R. Leo: Techniques for Nuclear and Particle Physics Experiments: A How-to Approach (Springer-Verlag, 1994) 2nd ed. https://doi.org/10.1007/978-3-642-57920-2
12 M. R. Rezaie, A. Negarestani, M. Sohrabi, S. Mohammadi, and D. Afzali: J. Radioanal. Nucl. Chem. **293** (2012) 39. https://doi.org/10.1007/s10967-012-1706-1
13 S. Matsumoto, Y. Kaneda, and A. Ito: Ceram. Int. **46** (2020) 1810. https://doi.org/10.1016/j.ceramint.2019.09.156
14 A. Ito and Y. Morishita: Mater. Lett. **258** (2020) 126817. https://doi.org/10.1016/j.matlet.2019.126817
15 S. Matsumoto and A. Ito: Opt. Mater. Express **10** (2020) 899. https://doi.org/10.1364/OME.386425
16 P. Zhao, A. Ito, and T. Goto: Surf. Coat. Technol. **235** (2013) 273. https://doi.org/10.1016/j.surfcoat.2013.07.048
17 H. Aida, R. Watanuki, and A. Ito: Mater. Lett. **276** (2020) 128228. https://doi.org/10.1016/j.matlet.2020.128228
18 K. Kato, R. Watanuki, and A. Ito: Mater. Lett. **274** (2020) 128046. https://doi.org/10.1016/j.matlet.2020.128046
19 A. Ito, H. Kadokura, T. Kimura, and T. Goto: J. Alloys Compd. **489** (2010) 469. https://doi.org/10.1016/j.jallcom.2009.09.088
20 Y. Fujimoto, T. Yanagida, H. Yagi, T. Yanagidani, and V. Chani: Opt. Mater. **36** (2014) 1926. https://doi.org/10.1016/j.optmat.2014.06.019
21 L. Jia-Liang, W. Yun-Tao, and R. Guo-Hao: J. Inorg. Mater. **29** (2014) 1211. https://doi.org/10.15541/jim20140145
22 P. Douissard, T. Martin, F. Riva, Y. Zorenko, T. Zorenko, K. Paprocki, A. Fedorov, P. Bilski, and A. Twardak: IEEE Trans. Nucl. Sci. **63** (2016) 1726. https://doi.org/10.1109/TNS.2016.2565731
23 Y. Zorenko, A. Voloshinovskii, I. Konstankevych, V. Kolobanov, V. Mikhailin, and D. Spassky: Radiat. Meas. **38** (2004) 677. https://doi.org/10.1016/j.radmeas.2004.02.009